DNA nanopore translocation in glutamate solutions

C. Plesa, N. van Loo and C. Dekker*

Nanopore experiments have traditionally been carried out with chloride-based solutions. Here we introduce silver/silver-glutamate-based electrochemistry as an alternative, and study the viscosity, conductivity, and nanopore translocation characteristics of potassium-, sodium-, and lithium-glutamate solutions. We show that it has a linear response at typical voltages and can be used to detect DNA translocations through a nanopore. The glutamate anion also acts as a redox-capable thickening agent, with high-viscosity solutions capable of slowing down the DNA translocation process by up to 11 times, with a corresponding 7 time reduction in signal. These results demonstrate that glutamate can replace chloride as the primary anion in nanopore resistive pulse sensing.

Introduction

Solid-state nanopores constitute an emerging biophysical technique which has been used to study DNA,[1] protein,[2] and DNA–protein complexes.[3–5] Although this area has been primarily pushed by the promise of its use for low-cost sequencing of long nucleic acid polymers, many other applications have opened up. Numerous studies have been published on methods to improve various aspects of this technique with different pore types,[6,7] membrane materials,[8–11] new salts,[12,13] and passivation techniques.[14,15] Although central to their operation, alternative electrochemical reactions for detecting the ionic current have not been pursued. In this study we introduce a novel electrochemical reaction based on glutamate (Glu) anions and demonstrate its potential for studying DNA translocations through solid-state nanopores. This approach provides a way to avoid the use of chloride and slow down the translocation velocity using high-viscosity solutions. Some of the previous attempts to slow down the DNA translocation process[16] have utilized thickening agents such as glycerol.[17,18] In this study we introduce the concept of redox capable thickening agents, which simultaneously increase the solution viscosity and participate in the electrochemical ionic current readout.

We first provide a brief overview of the solid-state nanopore method. Nanopores are typically fabricated in a 20 nm thick free-standing SiN membrane by focusing an electron beam on the membrane using a transmission electron microscope (TEM).[19] This allows simultaneous *in situ* imaging of the pore as it is being created. Membranes with pores are subsequently placed in a flow cell such that it separates two aqueous reservoirs filled with salt solution, as shown in Fig. 1a. Chlorinated silver electrodes are placed into the solution on each side and an electric potential is applied. The resulting ionic current is measured with a low-noise amplifier. Since DNA is negatively charged, it is electrophoretically driven through the nanopore. When a DNA molecule passes through the pore it causes a transient drop in the ionic current, since the molecule reduces the pore volume normally used by ions for transport. The duration of the blockade can be related to the length of the polymer, while the amplitude of the blockade is proportional to the volume of the molecule currently in the pore constriction.

We now address the electrochemistry used for the ionic current detection. In the typical silver/silver-chloride based electrochemistry, a chlorinated silver wire is placed in a chloride-salt-based solution and an electric potential is applied. At the anode, chloride ions are oxidized into solid-phase silver chloride through the reaction $Ag(s) + Cl^-(aq) \rightarrow AgCl(s) + e^-$ while at the cathode, silver chloride is reduced and chloride ions are released into the solution *via* the reaction $AgCl(s) + e^- \rightarrow Ag(s) + Cl^-(aq)$. The measured ionic current is linear with respect to the applied voltage at potentials below 1 V. The ease of electrode preparation, made by placing a silver wire in a bleach solution, makes this a simple and effective experimental approach. With only one exception, all nanopore publications that we are aware of use silver-chloride based electrochemistry together with either alkali metal halide solutions (LiCl,[12] NaCl,[3] KCl,[14] RbCl,[20] and

Department of Bionanoscience, Kavli Institute of Nanoscience, Delft University of Technology, Lorentzweg 1, 2628 CJ Delft, The Netherlands.
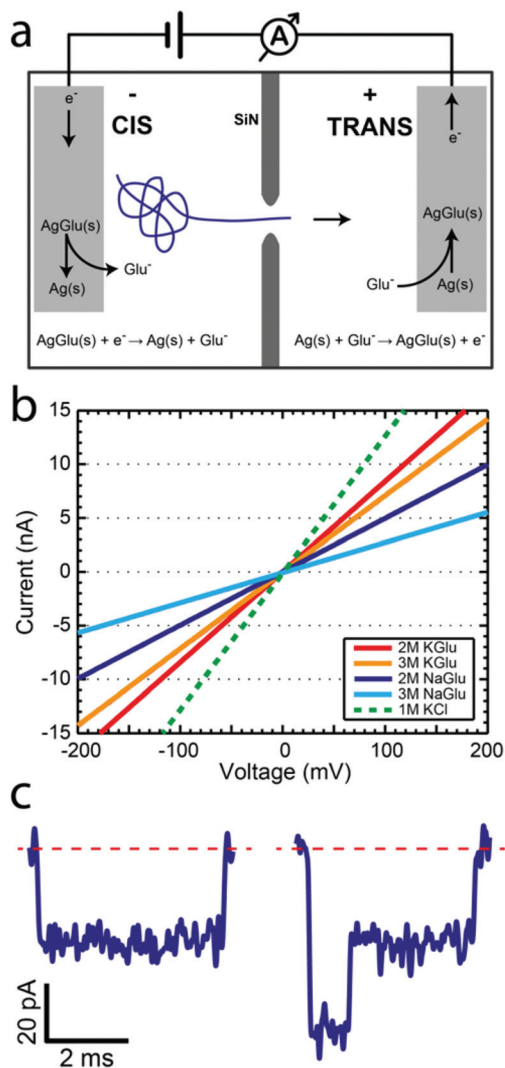*E-mail: c.dekker@tudelft.nl*

Fig. 1 (a) Schematic illustration of the nanopore setup with the redox reactions occurring at each electrode. (b) The current voltage response for 20 nm pores is observed to be linear over the range from −800 mV to 800 mV for NaGlu and KGlu at all tested concentrations. The open pore conductance is higher for KGlu solutions compared to NaGlu. For both salts, the pore conductance is higher at 2 M compared to 3 M concentration. The open pore conductance of 1 M KCl is also shown as a dashed line. (c) Typical translocation events for a 20.7 kbp linear DNA molecule observed in a 16 nm pore and 3 M KGlu at 100 mV. The dashed red line is the open pore current baseline.

CsCl[21]) or organic-salts (BMIM-Cl[13]), with chlorine always as the halogen constituent. The only non-chloride electrochemistry nanopore study looked at ionic liquids using platinum electrodes.[22]

L-Glutamic acid (Glu) plays a fundamental role in biology as one of the amino acids used in protein synthesis. In many organisms glutamate, not chloride, is the major intracellular anion.[23] Although many of its properties have been studied in detail, we are not aware of any literature on non-enzymatic glutamate-based electrochemistry. In 1974, an article by Tabei

et al.[24] described a method for making printed circuits through the photolysis of silver glutamate. From this work, we know that silver glutamate is a stable, albeit photosensitive, solid-phase compound, much like silver chloride.

We hypothesized that glutamate could be used to replace the chloride in the electrochemical reactions used in the nanopore studies. Analogous to the silver chloride case, we expect similar electrochemical reactions to take place at the anode

$$Ag(s) + Glu^-(aq) \rightarrow AgGlu(s) + e^- \qquad (1)$$

and the cathode

$$AgGlu(s) + e^- \rightarrow Ag(s) + Glu^-(aq). \qquad (2)$$

In this way, glutamate could be used as a redox-capable thickening agent to increase the viscosity of a solution while still maintaining the required electrochemistry.

Results

We now show that glutamate solutions produce a linear current–voltage response and can be used for detecting DNA nanopore translocations. We prepared silver glutamate electrodes by electrolysis of a 99.99% silver wire (anode) and platinum wire (cathode) in a concentrated 3 M potassium glutamate solution. These electrodes were then used, following standard procedures, in solid-state nanopore experiments. Fig. 1b shows the typical current–voltage curves observed for potassium glutamate (KGlu) and sodium glutamate (NaGlu) solutions at 2 M and 3 M concentrations in 20 nm pores. We have also included a typical response observed for 1 M KCl (dashed green line) for comparison. The IV responses were observed to be linear in the tested range of −800 mV to 800 mV. Additionally, the open pore conductance was observed to be higher at 2 M compared to 3 M, in both KGlu and NaGlu, as explained below while discussing the conductivity measurements. The open pore conductance can be related to several physical characteristics of the pore and the solution using[25]

$$G = \sigma \left[\frac{4l}{\pi d^2} + \frac{1}{d} \right]^{-1} \qquad (3)$$

where l is the membrane thickness, d is the pore diameter, and σ is the solution conductivity. Upon addition of a DNA solution to the flow cell, typical DNA translocation events could be observed in the current trace, as shown in Fig. 1c. These results demonstrate the feasibility of using glutamate-based salts for nanopore experiments.

To understand the pore conductance, we measured the conductivity of concentrated solutions of glutamate salts. Fig. 2a shows the conductivity at 23 °C as a function of concentration for KGlu, NaGlu, and LiGlu, alongside literature values[26] for KCl, NaCl, and LiCl at 25 °C. The maximum concentrations tested were limited by the solubility of the salts which were found to be around 1 M for LiGlu, 3.5 M for KGlu, and 3.3 M
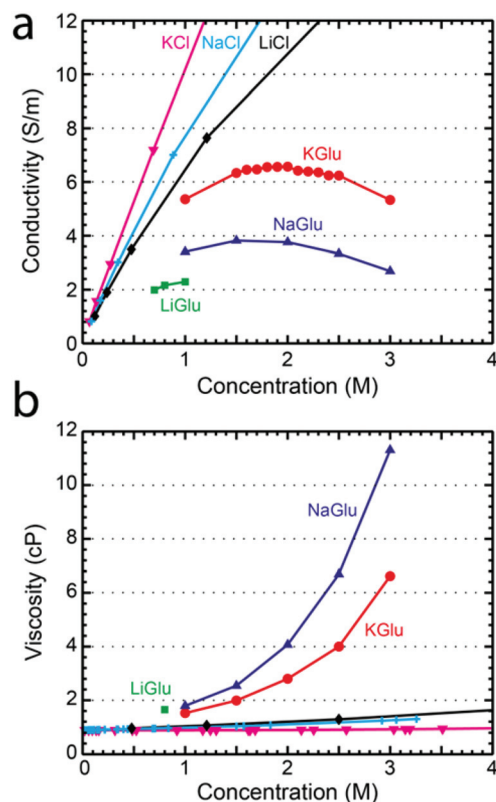
Fig. 2 (a) The conductivity of the glutamate solutions is lower than the equivalent chloride solutions and reaches a maximum between 1.5 M and 2 M. LiGlu could not be dissolved at concentrations above 1 M. (b) The viscosity of glutamate solutions can be significantly higher than the corresponding chloride solutions demonstrating their potential advantage as thickening agents.

in a higher drag force and a longer translocation time. In Fig. 2b the viscosity of LiGlu, KGlu, and NaGlu is shown as a function of solution concentration alongside literature values for KCl,[27] NaCl,[27] and LiCl[28] at 25 °C. As expected, the glutamate solutions have a significantly higher viscosity than the chloride solutions at the same concentration. We measured a viscosity of 2.8 cP and 6.6 cP for KGlu at 2 M and 3 M, and even higher viscosities of 4.1 cP and 11.3 cP, respectively, for NaGlu. The larger viscosities of the glutamate solutions compared to the chloride solutions can be explained by the much larger size of the glutamate (MW 147.13 g mol^{-1}) anion compared to chloride (MW 35.45 g mol^{-1}) and highlight its potential as a thickening agent.

Finally, we studied the characteristics of DNA translocation through nanopores in high concentration glutamate solutions to see how much the translocation velocity and conductance blockade were reduced. Linear 20.7 kbp DNA molecules were translocated through nanopores in 1 M, 2 M, and 3 M solutions of KGlu and NaGlu at 100 mV. Fig. 3a shows a typical heat plot showing the event's conductance blockade and translocation time in 2 M KGlu and a 20 nm pore. As expected from the viscosity measurements, events were slower in NaGlu compared to KGlu, as shown in Fig. 3b. In 2 M and 3 M KGlu, events had a 3.3× and 5.8× longer translocation time relative to 1 M KCl, while the translocation in 3 M NaGlu took 11.3× longer. The price paid for this slower translocation is a reduction in the blockade signal, as already observed in the conductivity measurements. In Fig. 3c we show the DNA conductance blockade in 1 M, 2 M, and 3 M glutamate salt solutions. We observe blockade amplitudes of 0.1, 0.35, and
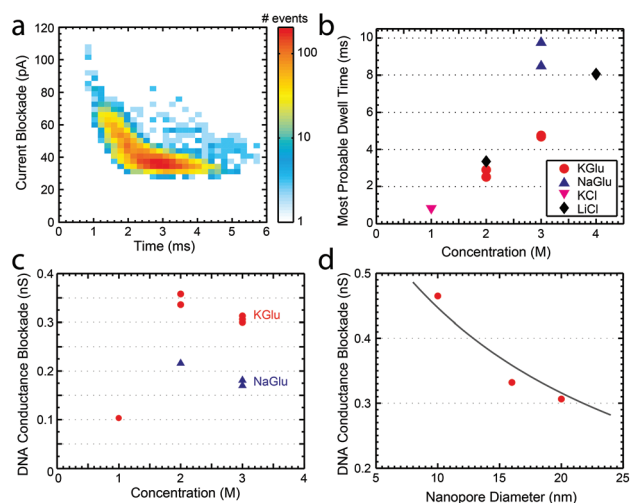
for NaGlu. The conductivity of KGlu was observed to be significantly higher than NaGlu, with values for KGlu of 6.57 S m^{-1} and 5.33 S m^{-1} at 2 M and 3 M compared to 3.76 S m^{-1} and 2.69 S m^{-1}, respectively, for NaGlu. The conductivities of both solutions were observed to have maxima, which was around 2.0 for KGlu and 1.7 for NaGlu. This is a common phenomenon at very high electrolyte concentrations and is attributed to the small inter-ionic separations which lead to strong ion–ion interactions that begin to reduce the conductivity of solutions above a certain concentration. Since we would like to maximize the ionic current signal, larger conductivities are desired and these measurements reveal that KGlu is preferable over NaGlu. As expected, the conductivities observed for the glutamate solutions were smaller than the corresponding chloride solutions at the same concentrations.

We also investigated the viscosity of glutamate salt solutions, relevant for the translocation speed of traversing molecules. A Brookfield DV2TLVCP Wells-Brookfield cone/plate viscometer was used to measure the viscosities of KGlu, NaGlu, and LiGlu at 23 °C. Viscosity is an important parameter in nanopore measurements since increasing viscosity results

Fig. 3 (a) Heat plot showing the conductance blockade and translocation time of 20.7 kbp DNA translocating through a 20 nm pore in 2 M KGlu. (b) The most probable dwell times observed for 20.7 kbp DNA at 100 mV in a variety of buffers. (c) DNA conductance blockade of 1 M, 2 M, and 3 M solutions of KGlu and NaGlu at 100 mV in 20 nm pores. (d) DNA conductance blockade in 3 M KGlu as a function of the pore diameter. The solid line is a fit to the geometric model of Kowalczyk et al.[25]

0.31 nS in 1 M, 2 M, and 3 M KGlu, which are around 12.5×, 3.6×, and 4× smaller than the DNA blockade in 1 M KCl (1.25 nS). This becomes worse for the NaGlu, with blockades of 0.22 nS and 0.18 nS, respectively. One common approach to increase the conductance blockade is to decrease the diameter of the nanopores used. Fig. 3d shows the DNA blockade for 3 M KGlu in 10, 16, and 20 nm pores. When the pore diameter is reduced from 20 nm to 10 nm we observe a 1.5× increase in the DNA blockade, to 0.47 nS. The observed trend can be fitted with a simple geometric model[25] (solid line in Fig. 3d) based on eqn (3). These DNA translocation experiments demonstrate the viability of using glutamate-based solutions for nanopore measurements.

Conclusions

In this study we have demonstrated that glutamate-based electrochemistry can replace traditional chloride-based reactions for use in nanopore measurements. Potassium glutamate provides a higher conductivity, compared to sodium glutamate, with a maximum of 6.57 S m^{-1} at around 2 M concentration. The use of lithium glutamate is limited by its maximum solubility of around 1 M. DNA translocation through glutamate solutions can be slowed down by 3.3× to 11.3× relative to 1 M KCl, while the conductance blockade signal is reduced by 3.6× and 7× respectively. These numbers are similar to those of a study carried out by adding glycerol into 1.5 M KCl solutions.[17] There, a 5.3× increase in the viscosity resulted in a 4.4× increase in the translocation time and a 3.1× decrease in the blockade amplitude, relative to the values for 1.5 M KCl. In addition to slowing down DNA translocation, the use of glutamate instead of chloride may provide a better environment for gold electrodes in three terminal devices.

Methods

Free standing SiN membranes were fabricated by using trans-chip illumination lithography.[29] Pores were drilled with a Philips CM200-FEG TEM. Ionic currents were measured with an Axopatch 200B and digitized at 500 kHz. Signals were subsequently analysed with the Transalyzer Matlab package.[30] All solutions contained 10 mM Tris at pH 8 and 1 mM EDTA. Potassium glutamate, sodium glutamate, and L-glutamic acid were purchased from Sigma-Aldrich (St. Louis, MO, USA). Lithium glutamate was made by Tocris Bioscience (Bristol, UK) following a procedure similar to the one described by Wiesbrock et al.[31] Briefly high purity L-α-glutamic acid was dissolved in HPLC grade water, after which an equivalent amount of lithium hydroxide was added. The resulting clear solution was then freeze dried to yield the solid salt. The product was characterized with micro analysis, infrared spectroscopy, proton NMR, and mass spectrometry. High purity silver and platinum wires were purchased from Advent Research Materials (Oxford, UK).

References

1 M. Wanunu, *Phys. Life Rev.*, 2012, **9**, 125–158.
2 C. Plesa, S. W. Kowalczyk, R. Zinsmeester, A. Y. Grosberg, Y. Rabin and C. Dekker, *Nano Lett.*, 2013, **13**, 658–663.
3 A. T. Carlsen, O. K. Zahid, J. A. Ruzicka, E. W. Taylor and A. R. Hall, *Nano Lett.*, 2014, **14**, 5488–5492.
4 M. Langecker, A. Ivankin, S. Carson, S. R. M. Kinney, F. C. Simmel and M. Wanunu, *Nano Lett.*, 2015, **15**, 783–790.
5 C. Plesa, J. W. Ruitenberg, M. J. Witteveen and C. Dekker, *Nano Lett.*, 2015, **15**, 3153–3158.
6 L. J. Steinbock, O. Otto, C. Chimerel, J. Gornall and U. F. Keyser, *Nano Lett.*, 2010, **10**, 2493–2497.
7 E. A. Heins, Z. S. Siwy, L. A. Baker and C. R. Martin, *Nano Lett.*, 2005, **5**, 1824–1829.
8 J. Larkin, R. Henley, D. C. Bell, T. Cohen-Karni, J. K. Rosenstein and M. Wanunu, *ACS Nano*, 2013, **7**, 10121–10128.
9 B. M. Venkatesan, A. B. Shah, J.-M. Zuo and R. Bashir, *Adv. Funct. Mater.*, 2010, **20**, 1266–1275.
10 G. F. Schneider, S. W. Kowalczyk, V. E. Calado, G. g. Pandraud, H. W. Zandbergen, L. M. K. Vandersypen and C. Dekker, *Nano Lett.*, 2010, **10**, 3163–3167.
11 K. Liu, J. Feng, A. Kis and A. Radenovic, *ACS Nano*, 2014, **8**, 2504–2511.
12 S. W. Kowalczyk, D. B. Wells, A. Aksimentiev and C. Dekker, *Nano Lett.*, 2012, **12**, 1038–1044.
13 R. S. S. de Zoysa, D. A. Jayawardhana, Q. Zhao, D. Wang, D. W. Armstrong and X. Guan, *J. Phys. Chem. B*, 2009, **113**, 13332–13336.
14 E. C. Yusko, J. M. Johnson, S. Majd, P. Prangkio, R. C. Rollings, J. Li, J. Yang and M. Mayer, *Nat. Nanotechnol.*, 2011, **6**, 253–260.
15 G. F. Schneider, Q. Xu, S. Hage, S. Luik, J. N. H. Spoor, S. Malladi, H. Zandbergen and C. Dekker, *Nat. Commun.*, 2013, **4**.
16 B. Luan, G. Stolovitzky and G. Martyna, *Nanoscale*, 2012, **4**, 1068–1077.
17 D. Fologea, J. Uplinger, B. Thomas, D. S. McNabb and J. Li, *Nano Lett.*, 2005, **5**, 1734–1737.
18 B. Luan, D. Wang, R. Zhou, S. Harrer, H. Peng and G. Stolovitzky, *Nanotechnology*, 2012, **23**, 455102.
19 A. J. Storm, J. H. Chen, X. S. Ling, H. W. Zandbergen and C. Dekker, *Nat. Mater.*, 2003, **2**, 537–540.

20 M. F. Breton, F. Discala, L. Bacri, D. Foster, J. Pelta and A. Oukhaled, *J. Phys. Chem. Lett.*, 2013, **4**, 2202–2208.

21 G. V. Soni, A. Singer, Z. Yu, Y. Sun, B. McNally and A. Meller, *Rev. Sci. Instrum.*, 2010, 81.

22 M. Davenport, A. Rodriguez, K. J. Shea and Z. S. Siwy, *Nano Lett.*, 2009, **9**, 2125–2128.

23 S. Cayley, B. A. Lewis, H. J. Guttman and M. T. Record Jr., *J. Mol. Biol.*, 1991, **222**, 281–300.

24 H. Tabei, S. Nara and K. Matsuyama, *J. Electrochem. Soc.*, 1974, **121**, 67–69.

25 S. W. Kowalczyk, A. Y. Grosberg, Y. Rabin and C. Dekker, *Nanotechnology*, 2011, **22**, 315101.

26 G. D. Fasman, in *Practical handbook of biochemistry and molecular biology*, ed. G. D. Fasman, CRC Press, Boca Raton, FL, 1989.

27 Z. Hai-Lang and H. Shi-Jun, *J. Chem. Eng. Data*, 1996, **41**, 516–520.

28 I. M. Abdulagatov, A. B. Zeinalova and N. D. Azizov, *J. Mol. Liq.*, 2006, **126**, 75–88.

29 X. J. A. Janssen, M. P. Jonsson, C. Plesa, G. V. Soni, C. Dekker and N. H. Dekker, *Nanotechnology*, 2012, **23**, 475302.

30 C. Plesa and C. Dekker, *Nanotechnology*, 2015, **26**, 084003.

31 F. Wiesbrock and H. Schmidbaur, *CrystEngComm*, 2003, **5**, 262–264.